AD-A110 741 FLORIDA UNIV GAINESVILLE F/6 11/4
STUDIES ON THE FRACTURE MECHANISMS IN PARTIALLY PENETRATED FILA--ETC(U)
DEC 81 R L SIERAKOWSKI, C A ROSS, L E MALVERN DAAG29-79-G-0007
UNCLASSIFIED ARO-15989.7-E NL

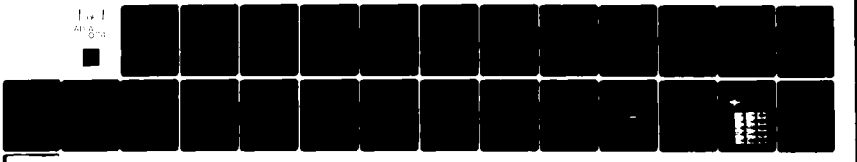

END
DATE FILMED
3-82
DTIC

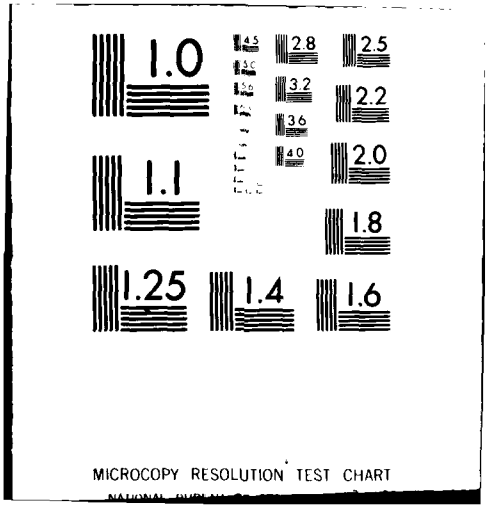
1.0
1.1
1.25
1.4
1.6
1.8
2.0
2.2
2.5
2.8
3.2
3.6
4.0
4.5
5.0
5.6
MICROCOPY RESOLUTION TEST CHART

UNCLASSIFIED
SECURITY CLASSIFICATION OF THIS PAGE (When Data Entered)

LEVEL I

12

REPORT DOCUMENTATION PAGE

READ INSTRUCTIONS BEFORE COMPLETING FORM

1. REPORT NUMBER	2. GOVT ACCESSION NO.	3. RECIPIENT'S CATALOG NUMBER
15989.7-E	AD-A110 741	

4. TITLE (and Subtitle)

Studies on the Fracture Mechanisms in Partially Penetrated Filament Reinforced Laminated Plates

5. TYPE OF REPORT & PERIOD COVERED

Final:
1 Dec 78 - 30 Nov 81

6. PERFORMING ORG. REPORT NUMBER

7. AUTHOR(s)

R. L. Sierakowski
C. A. Ross
L. E. Malvern

8. CONTRACT OR GRANT NUMBER(s)

DAAG29 79 G 0007

9. PERFORMING ORGANIZATION NAME AND ADDRESS

University of Florida
Gainesville, FL 32611

10. PROGRAM ELEMENT, PROJECT, TASK AREA & WORK UNIT NUMBERS

11. CONTROLLING OFFICE NAME AND ADDRESS

U. S. Army Research Office
Post Office Box 12211
Research Triangle Park, NC 27709

12. REPORT DATE

Dec 81

13. NUMBER OF PAGES

24

14. MONITORING AGENCY NAME & ADDRESS (if different from Controlling Office)

15. SECURITY CLASS. (of this report)

Unclassified

15a. DECLASSIFICATION/DOWNGRADING SCHEDULE

16. DISTRIBUTION STATEMENT (of this Report)

Approved for public release; distribution unlimited.

17. DISTRIBUTION STATEMENT (of the abstract entered in Block 20, if different from Report)

NA

18. SUPPLEMENTARY NOTES

The view, opinions, and/or findings contained in this report are those of the author(s) and should not be construed as an official Department of the Army position, policy, or decision, unless so designated by other documentation.

19. KEY WORDS (Continue on reverse side if necessary and identify by block number)

fracture properties
impact loading
composite materials
fiber reinforced composites
laminates
glass/epoxy composites
penetration

20. ABSTRACT (Continue on reverse side if necessary and identify by block number)

The overall objective of this program has been to obtain information on the fracture mechanisms occurring in centrally impacted composite plate configurations in order to establish basic design guidelines from systematic studies on geometrically controlled glass/epoxy composite material systems. In addition, information generated on the values of the dynamic material properties determined from the program should be of immediate use in penetration mechanics codes requiring such data.

DD FORM 1 JAN 73 1473 EDITION OF 1 NOV 65 IS OBSOLETE

UNCLASSIFIED
SECURITY CLASSIFICATION OF THIS PAGE (When Data Entered)

AD A110741

DTIC FILE COPY

STUDIES ON THE FRACTURE MECHANISMS IN PARTIALLY PENETRATED FILAMENT REINFORCED LAMINATED PLATES

FINAL

R.L. SIERAKOWSKI
C.A. ROSS
L.E. MALVERN

DECEMBER 31, 1981

U.S. ARMY RESEARCH OFFICE

DAAG29-79-G-0007

UNIVERSITY OF FLORIDA

TABLE OF CONTENTS

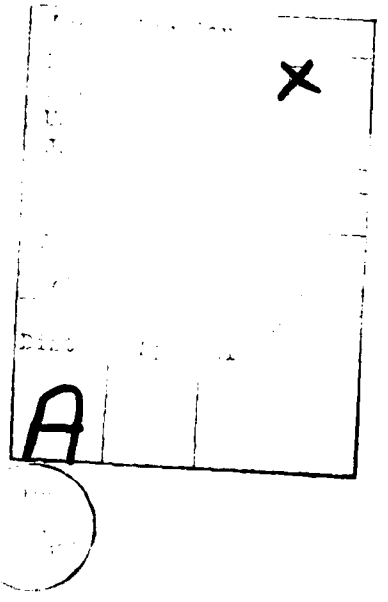

List of Figures

(I) Statement of Problem Studied

The ability of structural components to withstand short duration transient loadings is related to the way in which the stress and deformation are transmitted through the material. This transmission may involve elastic stress waves, propagating plastic deformation zones, and/or propagating cracks. The transmitted stress waves can also produce considerable damage at locations far removed from the impact site, and propagating damage zones can spread the energy absorption over a large volume of the impacted body.

The prediction and control of the failure zones in material systems subjected to transient loading requires understanding of both the basic dynamic materials properties and the mechanisms by which stress and deformation propagate through the material. These problems are interrelated, since the dynamic materials properties must be determined experimentally under conditions of transient loading where the stress and deformation are not uniform throughout the test specimen, and of course the stress wave propagation, dispersion and attenuation depend upon the dynamic material properties. The spreading of damage zones may also involve fracture mechanics information.

The introduction of high strength filamentary type composite materials as primary and secondary members in structural applications has focused attention on the need to characterize their response behavior for a wide variety of loadings. Due to the anisotropy of these materials, the observed response can vary considerably as compared to monolithic materials for a given set of loadings.

To understand the response of filamentary composite materials to dynamic loadings a program investigating the fracture mechanisms in partially penetrated centrally impacted laminated plates has been conducted.

The investigation has been structured into three phases of study. Phase I has involved experimental studies on the effects on the fracture mechanisms of varying the impactor and plate configurations, including changes in impactor nose shape, impactor mass and length and variations in lamina stacking sequences. Phase II has dealt with recording the time history of the flexural waves occurring in impacted plates and studying the sequential delamination and crack propagation which develops during the transient event. Analytical models for obtaining quantitative information on the stresses generated in the flexural wave by using available computer codes and for estimating the threshold levels of shear stresses for interlaminar shear failure have been studied. The third phase of the study has examined the retained or residual strength and stiffness of the plates after impact, assessing the load bearing capacity of the surviving structural configuration.

The overall objective of this program has been to obtain information on the fracture mechanisms occurring in centrally impacted composite plate configurations in order to establish basic design guidelines from systematic studies on geometrically controlled glass/epoxy composite material systems. In addition, information generated on the values of the dynamic material properties determined from the program should be of immediate use in penetration mechanics codes requiring such data.

(II) Summary of Important Results

A brief summary of the important results obtained in the overall program is given below. The individual descriptions have been accompanied where appropriate with graphical schematics to enhance and emphasize the results obtained. Each summary also cites publications listed in Part III where more detailed descriptions of the results are reported.

(a) Impactor Nose Shape Effects (Publications 1 and 3)

All impact tests conducted in this phase of the study were performed using the gas gun assembly described in publication 1 of Section III. A $[0^\circ_5/90^\circ_5/0^\circ_5]$ stacking sequence was used as the principal laminate structure for the study. Plate specimens were fabricated from fiberglass/epoxy prepreg tapes* using an autoclave to control the pressure and the temperature during specimen fabrication.

Results indicate that hemispherical nose shapes produce a local crushing and a less developed front-face generator strip than blunt nose impactors, all other factors remaining equal. (See Figure 1). Sequential delamination mechanisms occur for all impactor nose shapes studied with little if any effect of the impactor nose shape apparent in the observed delaminated area versus kinetic energy plots. (See Figure 2). Thus, the apparent fracture surface areas follow a linear relation with little if any change of slope noted for the nose shapes tested. While the total delaminated area remains unchanged with nose shape, the delaminated area ratios between the two interfaces in the specimens change with impactor nose shape. Also the mean

---

*'Scotchply' Type 1003, 12" or 18" wide, B Stage tape, Resin content 36% by weight.

distance between transverse cracks developing at the back face was observed to be less than the mean transverse crack spacing at the front face with hemispherical nose shaped impactors while the reverse occurs in the case of blunt nosed impactors.

(b) Impactor Length/Mass Effects (Publications 1 and 4)

The longer/heavier impactors generally have longer contact times compared to the lighter and/or slower ones, (See Figure 3), with the short impactors often making multiple contacts. It appears, however, that only the first contact period is important in transferring energy from the impactor to the laminate. Measured contact times generally ranged from 200 to 1200 microseconds in duration. Also, somewhat longer contact times were observed for the blunt nosed type impactors as compared with the other nose shapes tested.

Changes in impactor length/mass do not appear to introduce deviations in the nature of the observed delamination or apparent fracture surface energy versus initial kinetic energy relation. That is, a linear relation exists between the aforementioned parameters in each case. The slope of the curve is, however, affected, with the larger impactors used in these tests producing a thirty percent higher fracture surface energy than the corresponding smaller sized impactors. A twenty five percent change in the threshold level at which the delamination event occurs was also noted in the case of the longer impactors. (See Figure 2). The large scatter for kinetic energy greater than 30J occurs in the velocity regime where the delaminations approach the specimen boundary.

(c) Geometric/Angle ply Orientation Effects (Publications 1 and 6)

Angle-ply composite specimens consisting of fifteen ply symmetric laminates with ply orientations of $(15^{\circ}_5/-15^{\circ}_5/15^{\circ}_5]$ and $[30^{\circ}_5/-30^{\circ}_5/30^{\circ}_5]$ were

fabricated and impacted by 2.54 cm blunt nosed impactors. Once again a linear relationship between the delamination area and initial impactor kinetic energy was noted with similar but skewed fracture patterns observed as compared to the cross-ply specimens observed (See Figure 4). The apparent delamination fracture surface energy was found to be lower than that measured for the cross-ply specimens. The threshold energy for development of delamination was found, however, to be higher for the angle-ply laminates than for the cross-ply specimens. (See Figure 5).

(d) Flexural Wave Propagation Measurements (Publication 2)

Dynamic Strain measurements using surface and embedded strain gages with different gage layouts have been used for cross-plied $[0^\circ_5/90^\circ_5/0^\circ_5]$ laminates to record wave forms, wave amplitudes, and strain rates. Impactors used in this study were 2.54 cm. in length with impact speeds of the order of 30-40 m/sec. Observed events occurring on the front [back] gages include, first the arrival of a small in-plane tensile wave at both gages followed by a tensil[e] [compressive] component of the flexural wave. This is followed by a larger compressive [tensile] component of the flexural wave. It is believed that the largest amplitude of the flexural wave is the most important factor related to the observed delamination occurring. The wave speed associated with the largest amplitude has been measured as approximately 300 m/sec in the 0° ply direction and 33 percent less in the 90° direction. Measured wave velocities of the leading flexural wave have agreed well with those calculated on the basis of known elastic constants. Embedded gages in the laminates have verified that the dominant wave measured has been the flexural wave. A typical record of the wave forms observed has been documented in the accompanying Figure 6. Further information on both measured and calculated flexural wave speeds can be found in publication 2.

(e) Generator Strip Formation (Publication 4)

Generator strip formation, as seen in the schematic for angle-ply laminates in Figure 4, appears to be a key factor in fracture initiation associated with delamination events occurring for impacts of the type described here. To establish bounds on the generator strip propagation speeds, a series of conductive strips of silver paint were applied at fixed interval distances to the surface of the $[0^{\circ}_5/90^{\circ}_5/0^{\circ}_5]$ laminates impacted by both short and long nosed impactors. (See Figure 7). The strips were connected to appropriate oscilloscope channels in such a way that voltage-time records could be independently obtained. (See Figure 8). A general decrease in the generator strip velocity was noted, with propagation initially occurring at about 600-700 m/sec and decreasing to 400-500 m/sec. As the impact speed increased the generator strip velocity also increased; however, for equal kinetic energy impact events there appears to be little difference in generator strip speed between the short and longer impactors tested. It is of interest to note that the generator strip formation velocity is approximately twice the delamination crack propagation velocity and that based upon test measurements the strip formation is completed within 100 microseconds after initial contact of the impactor. This is consistent with previous observations that the generator strip is the nucleation mechanism for the delamination cracks occurring in the specimens.

(f) Delamination Crack Propagation Speeds (Publication 4)

In order to measure the delamination crack propagation velocities occurring inside a composite laminate, a Nova Model 16-3 16 mm high speed camera was used. Since the glass-epoxy cross-ply laminates are semitransparent, high speed photos recording the impact event could be taken by illuminating the front side of the plate and filming the event from the

back side. A sequence of high speed photos taken for a 2.54 cm blunt nosed impactor contacting a cross-plied $[0^\circ_5/90^\circ_5/0^\circ_5]$ laminate at 74.5 m/sec. is shown in Figure 9. While the photocopy remains grainy compared to the original, it does serve to document and illustrate the sequence of delamination events as used in calculating the delamination crack propagation velocity. From the results obtained and the laminates studied it appears that the delamination cracks initiated at the first and second interfaces start and propagate simultaneously; however, the first crack stops before the second does. (See photos 13 and 15 of Figure 9). Also it appears that delamination crack propagation velocites are little affected by impactor velocity , length (mass), and nose shape. Based upon calculations made from the high speed photos, the delamination crack in the 90° direction at the first interface propagates initially at 300-400 m/sec and decreases to 200-300 m/sec during the period of observation, stopping at about 100 microseconds while the delamination crack generated in the 0° direction at the second interface propagates initially at about 400-500 m/sec. decreasing to 270-400 m/sec during the period of observation, and stopping at about 300 microseconds. The last velocity agrees with measurements taken on the largest-amplitude flexural wave propagation velocity measured by strain gage sensors. This has been construed as being further documentation that delamination is associated with the flexural wave. Inspection of the records of the impact event also document that transverse cracks and delamination cracks occur almost simultaneously.

(g) Transverse Cracks and Delaminations (Publication 3)

In the course of the impact studies reported here, observable transverse cracks in the direction of the surface fibers have been noted to develop on the front and back faces of the plate specimens impacted by blunt-nosed

impactors. These cracks extend along the full length of the specimen faces and appear to be evenly spaced (distributed) on the surface plies. The mean transverse crack distance (MTCD) has been found to be related to the impactor velocity as shown in Fig. 10, with MTCD decreasing with increase in impactor velocity. Also the impactor nose shape appears to be important as discussed in Section (II-a).

The threshold velocity for development of the transverse cracks appears to be independent of impactor type and is of the order of 23 m/sec. Above this velocity the MTCD is observed to decrease with increase in velocity. At the lower velocities the heavier/longer impactors, which have longer contact times, appear to produce a larger MTCD than the smaller impactors. At the higher velocities, however, there was no apparent effect on the MTCD from changing impactor mass.

(h) Residual Strength and Stiffness (Publication 6)

The residual strength of panels has been measured using static cylindrical bending tests in which the square plate, supported on two edges, has been loaded centrally by a wedge with a rounded edge.

In the major test series the two edges selected for support were chosen so that the plate was tested in the stronger orientation. That is, with the 0° direction defined as perpendicular to the supports and loading wedge, the outer ply fiber orientation θ satisfied $0° \leq \theta \leq 45°$. Both undamaged plates and plates damaged by impacts at various speeds by a blunt-ended impactor have been tested in order to obtain a measure of the degradation in strength and stiffness caused by the impacts for the different ply arrangements.

Three test series were run for assessing the effect of ply arrangement. The first series of tests used the stacking sequence $30^\circ_5/\phi^\circ_5/\ 30^\circ_5$, maintaining the outer fibers at $\phi = 30°$ while the core fiber orientation was changed in 15°

increments from $\phi = 0°$ to $\phi = 60°$. The second series used the sequence $\theta_5/(90°-\theta)_5/\theta_5$, keeping the core ply always at 90° relative to the outer ply and changing θ in 15° increments from 0° to 45°. The third series studied the effect of changing the number of plies in each lamina of a crossply arrangement, that is $[0°/90°/...]$, $[0^3_\circ/90^3_\circ/0^3_\circ]$ to $[0^5_\circ/90^5_\circ/0^5_\circ]$.

The first series of tests showed only a weak dependence on core orientation. The second series showed, as would be expected, a significant dependence of the undamaged plate strength on outer ply orientation, with the strongest plates having $\theta = 0°$. It appears that the outer fiber orientation also has the strongest effect on the residual strength of plates having a large amount of impact-induced damage, although this result is not so conclusive because of the limited number of tests. The third series showed that increasing the number of plies in the outermost lamina enhances both undamaged plate strength and residual strength relative to the undamaged strength in the glass/epoxy crossply system.

Stiffnes degradation from the impact damage was much less than the strength degradation, as measured in these three point bend tests. Detailed results are given in Publication No. 6.

(i) Interlaminar Shear Stress Analysis (Publication 6)

Two computer codes have been used in an attempt to obtain quantitative information on the stresses in the elastic flexural wave and estimates of the threshold levels of shear stress for interlaminar shear failure.

The first calculations used the DEPROP (Dynamic Elastic-Plastic Response of Plates) code. This calculated the elastic bending stresses for a loading simulating a central impact at 150 ft/sec, assuming no delamination or other failure. The code uses a classical laminated orthotropic plate theory, not including shear deformation effects. Shear stresses were then calculated by

integrating the stress equations of motion, using the bending stresses obtained from the plate theory solution.

Later calculations used the SAP IV code to solve the three dimensional elasticity equations for similar simulated impacts. This procedure calculated the shear stresses directly. The two methods gave reasonably good agreement for the maximum interlaminar shear stresses.

For a $[0_5^\circ/90_5^\circ/0_5^\circ]$ glass epoxy composite plate the SAP IV calculations showed a zone in the first interlaminar plane extending from the impacted region toward the boundary in the 0° direction, the fiber direction of the outer lamina, in which the shear stress component in that direction was large (exceeding the estimated interlaminar shear strength based on the manufacturers quoted shear strength for the matrix). The shear stress component in the 90° direction was small, and the extent of the high shear stress region was also small in the 90° direction. The elastic analysis by the SAP IV code also showed that the shear stress under the impact point was much higher for the top interlaminar plane than it was for the second interlaminar plane. The high shear stress regions for both analyses agreed qualitatively with the areas that were observed to be delaminated in the experiments.

(III) List of Publications and Technical Reports

1. "Experimental Impactor/Plate Configuration Interaction Studies of Impacted Glass Fiber-Reinforced Composite Laminates", N. Takeda, R. L. Sierakowski, L. E. Malvern, SAMPE Quarterly, Vol. 12, pp. 9-17, January 1981.
2. "Wave Propagation Experiments in Ballistically Impacted Composite Laminates", N. Takeda, R. L. Sierakowski, L. E. Malvern, Journal of Composite Materials, Vol. 15, pp. 157-174, March, 1981.
3. "Transverse Cracks in Glass/Epoxy Laminates Impacted by Projectiles", N. Takeda, R. L. Sierakowski, L. E. Malvern. Journal of Materials Science, Vol. 16, pp. 2008 - 2011, July, 1981
4. "Delamination Crack Propagation Studies of Ballistically Impacted Composite Laminates", N. Takeda, R. L. Sierakowski, C. A. Ross, L. E. Malvern. To be published in Experimental Mechanics.
5. "Microscopic Observations of Cross Sections of Impacted Composite Laminates", N. Takeda, R. L. Sierakowski, L. E. Malvern, To be published in Composites Technology.
6. "Studies on the Fracture Mechanisms in Partially Penetrated Filament Reinforced Laminated Plates," Technical Report No. 1, R. L. Sierakowski, L. E. Malvern, C. A. Ross under DAAG-79-G-007, University of Florida. To be published.

(IV) List of all Participating Scientific Personnel

Principal Investigators

R. L. Sierakowski

L. E. Malvern

C. A. Ross

H. W. Doddington

Participating Personnel

Carolyn C. Schauble, Asst. Engr., Computer Analyst

N. Takeda, Ph.D., August, 1980

S.A.M. Khalil, Ph.D., Candidate

Teresa J. Roberts, Undergraduate Assistant

D. Yarborough, Undergraduate Assistant

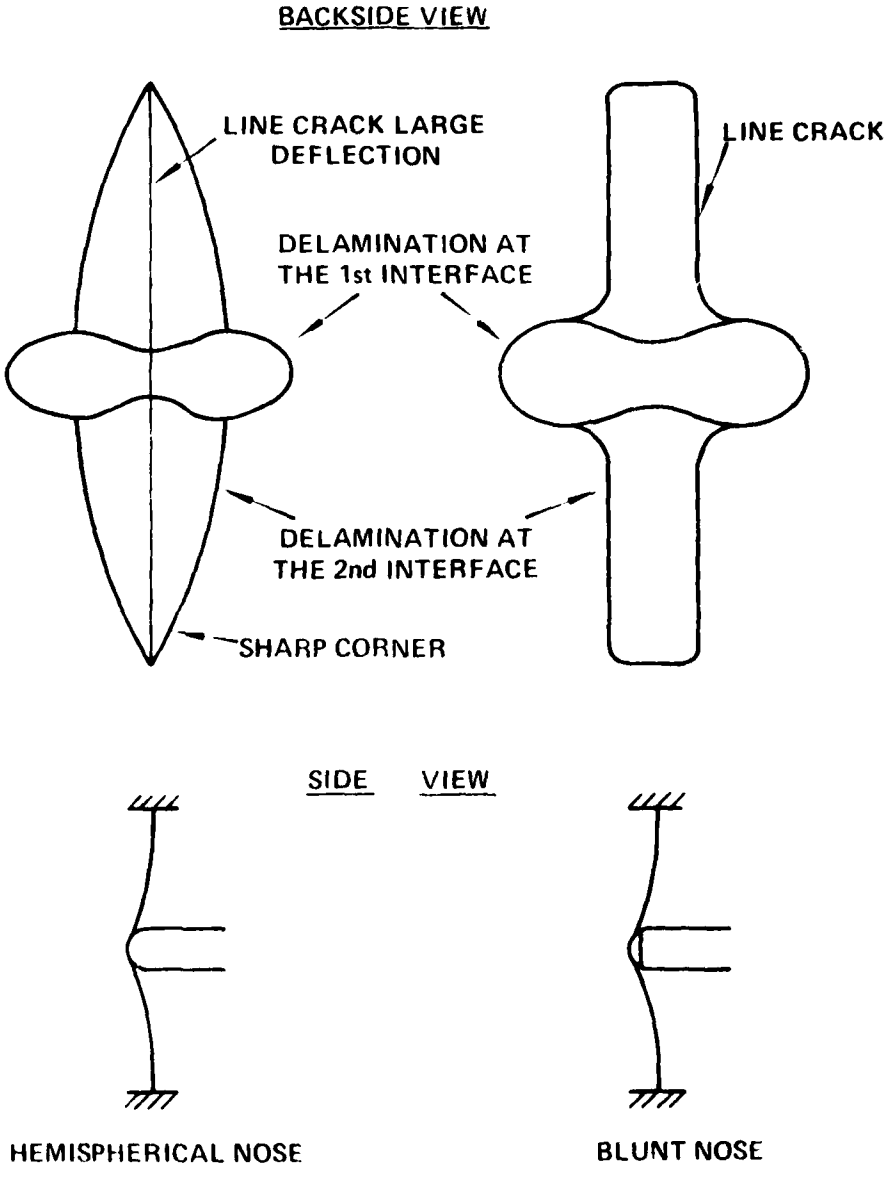

FIGURE 1. SCHEMATIC OF FRACTURE PATTERNS AND DEFORMATIONS OF LAMINATES IMPACTED BY TWO DIFFERENT NOSE SHAPE IMPACTORS

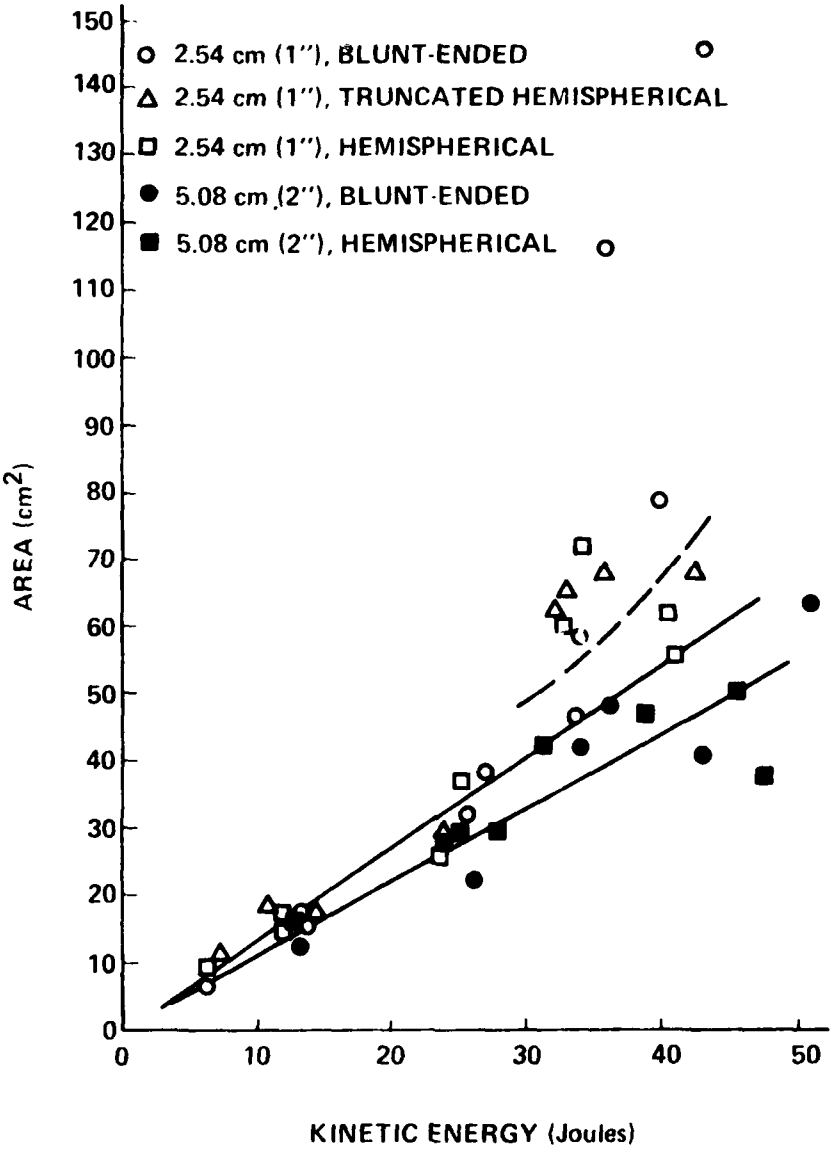

FIGURE 2. TOTAL DELAMINATION AREA VERSUS INITIAL IMPACTOR KINETIC ENERGY FOR $[(0^{\circ})_5/(90^{\circ})_5/(0^{\circ})_5]$ LAMINATES

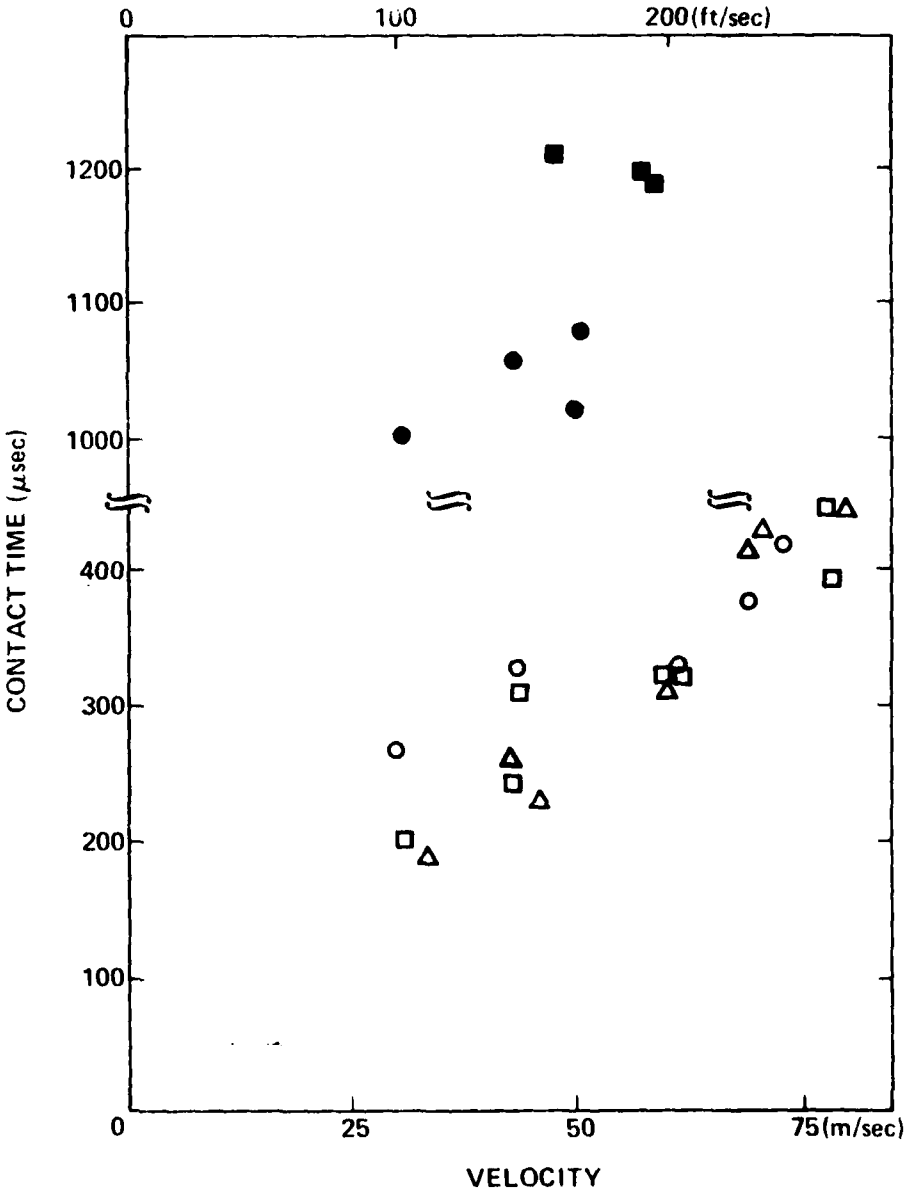

FIGURE 3. CONTACT TIME VERSUS IMPACTOR VELOCITY. (THE SAME SYMBOLS ARE USED AS IN FIG. 2)

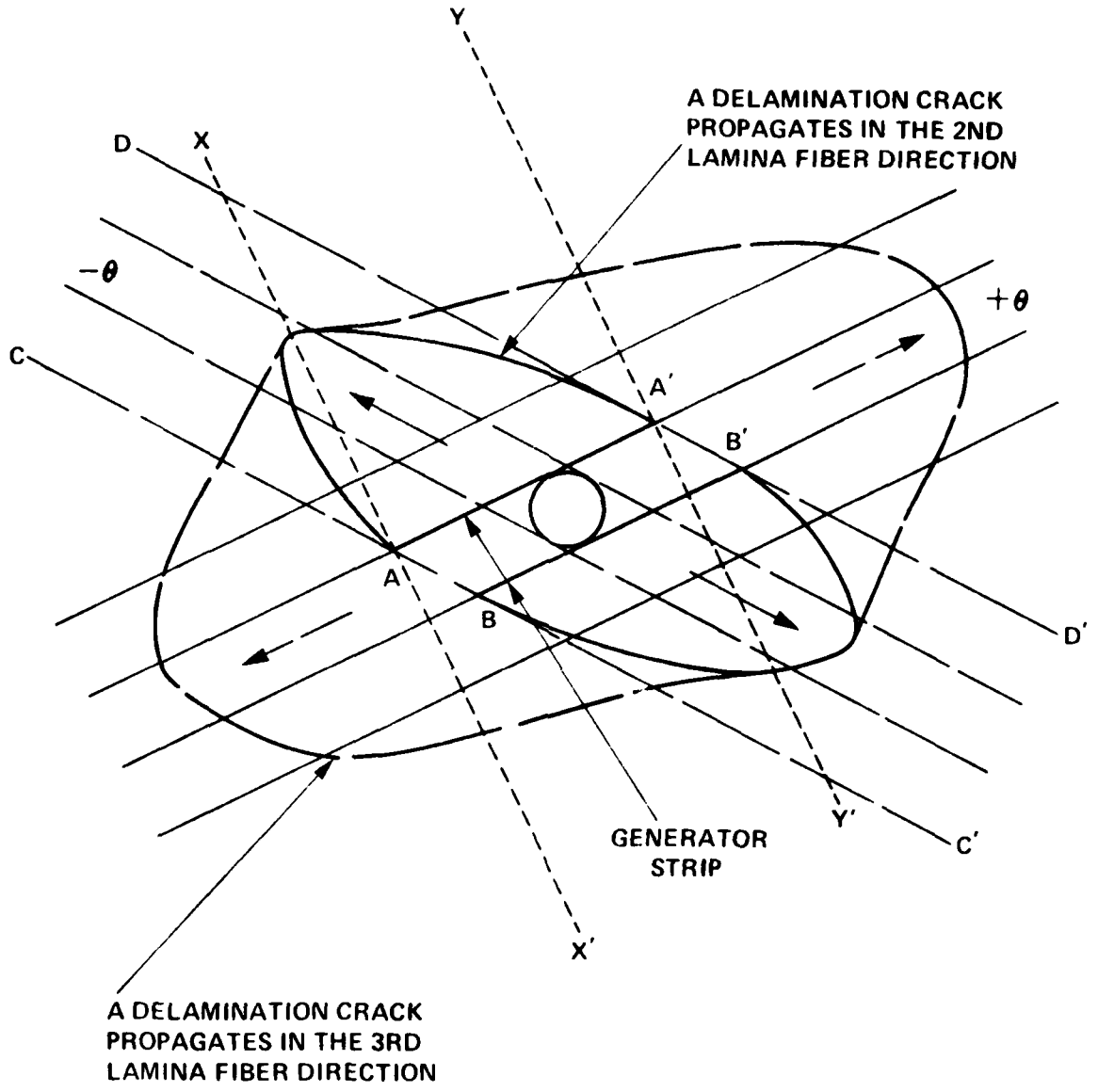

FIGURE 4. SCHEMATIC OF DELAMINATION PATTERN IN $[(+\theta)_5/(-\theta)_5/(+\theta)_5]$ ANGLE-PLY LAMINATES.

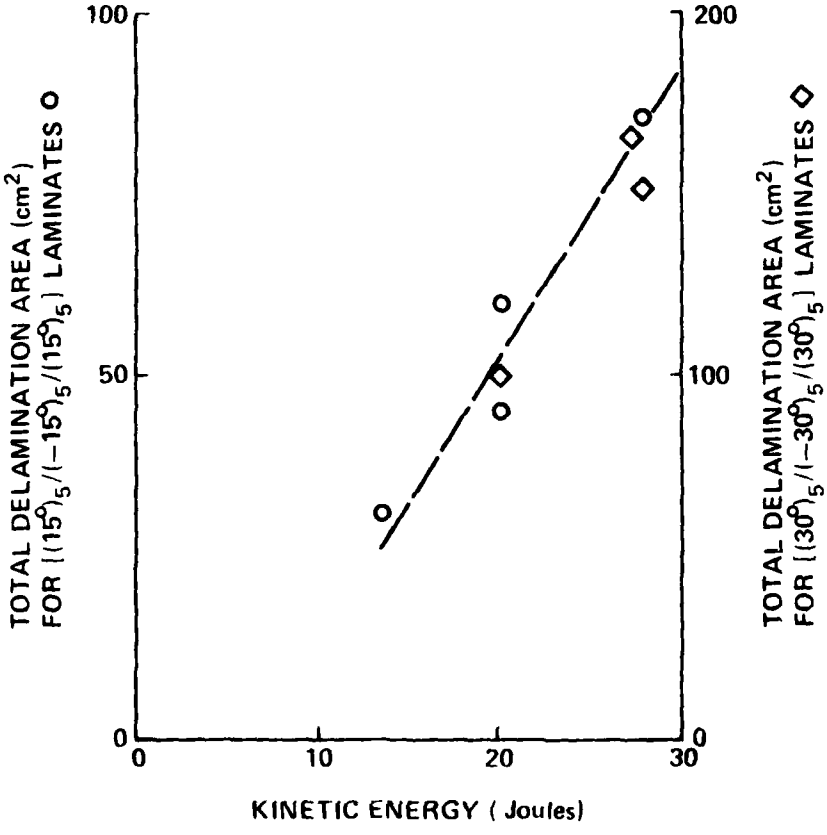

FIGURE 5. TOTAL DELAMINATION AREA VERSUS IMPACTOR KINETIC ENERGY FOR ANGLE–PLY LAMINATES.

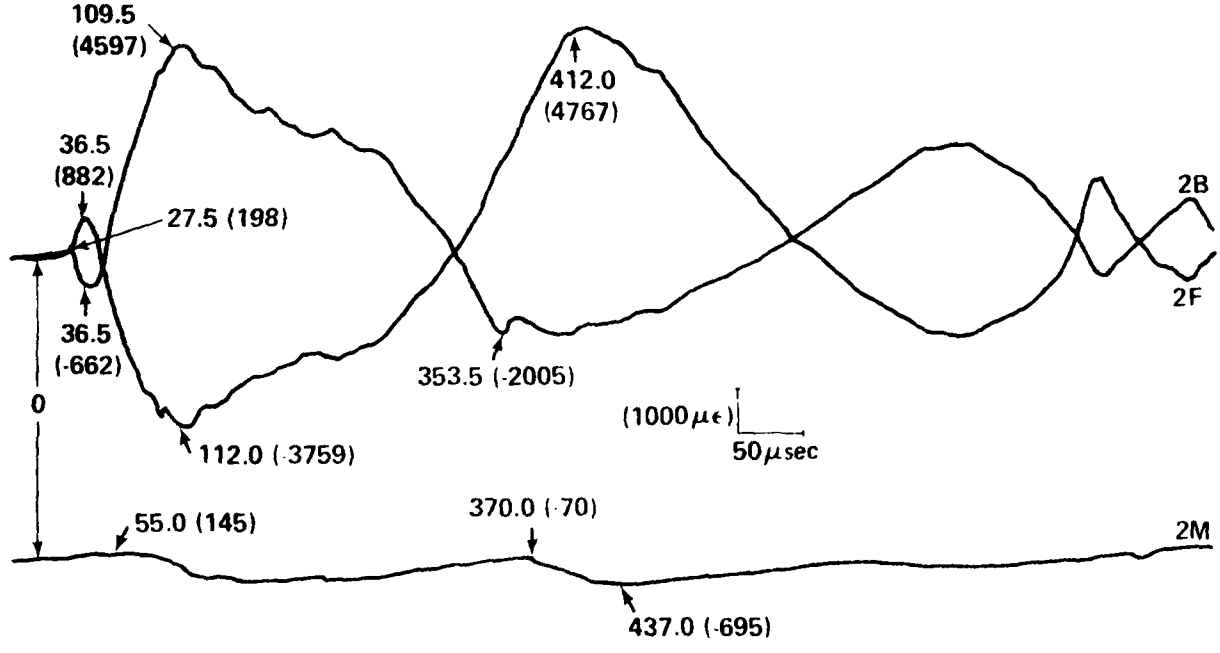

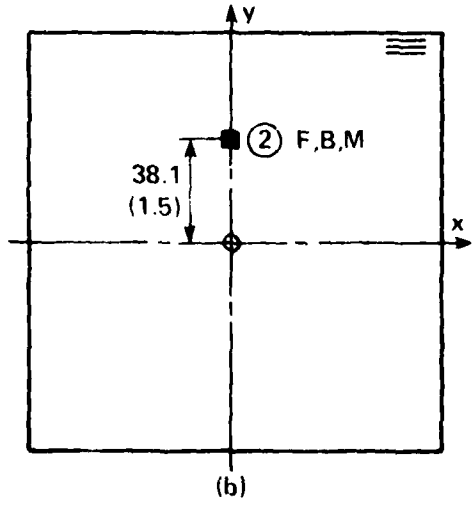

IMPACTOR VELOCITY
= 24.5m/sec (80.3ft/sec)

FIGURE 6. RECORDS FROM SURFACE AND EMBEDDED STRAIN GAGES IN 0° DIRECTION, OF AN IMPACTED $[(0^\circ)_5/(90^\circ)_5/(0^\circ)_5]$ GLASS/EPOXY LAMINATE. GAGES ARE ALL 38.1 mm FROM THE PLATE CENTER. M DENOTES EMBEDDED GAGES IN THE MID-PLANE OF THE LAMINATE.

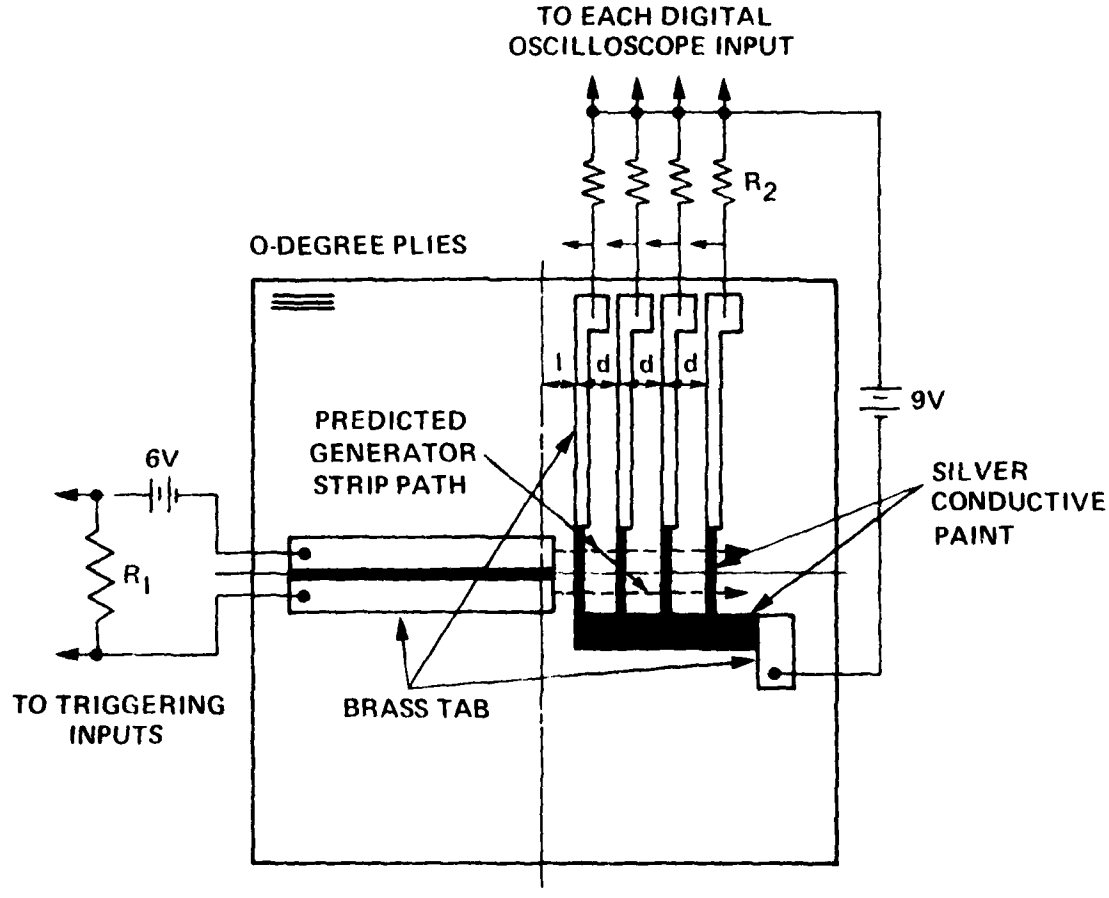

FIGURE 7. GENERATOR STRIP VELOCITY GAGE ARRANGEMENT
(l = 13 mm, d = 10 mm)

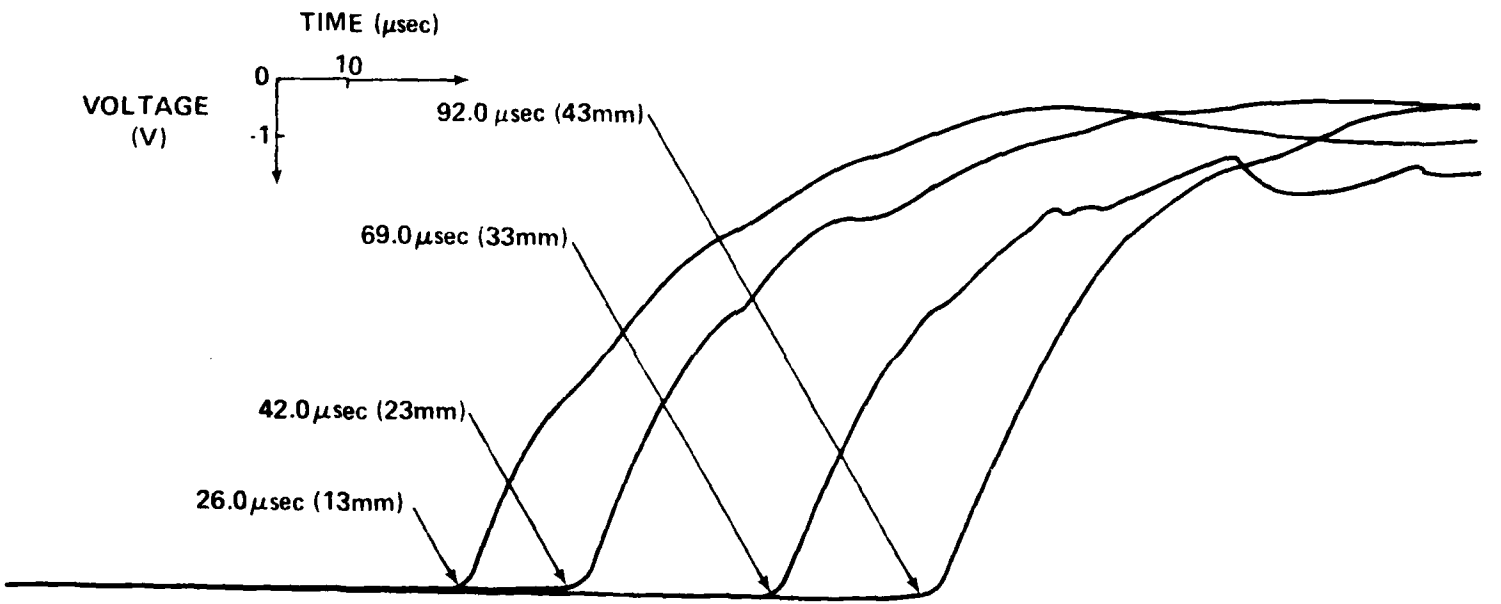

FIGURE 8. VOLTAGE–TIME RECORD OF GENERATOR STRIP FORMATION VELOCITY IN A LAMINATE IMPACTED BY A 2.54 cm BLUNT–NOSED IMPACTOR AT 70.3 m/s.

Figure 9.

Sequence of delamination crack propagation in a $[(0°)_5/(90°)_2/(0°)_5]$ laminate impacted by a 2.54 cm blunt-nosed impactor at 74.5 m/s (244.4 ft/s). 27.1 μs/frame.

Photos 1-7: Shadows of the impactor are coming towards the center of the target laminate. The impactor velocity can be calculated from the shadow velocity.

Photo 8: The impactor hits the target laminate.

Photo 9: Delamination cracks begin to propagate.

Photo 11: Both delamination cracks at the first and second interfaces propagate simultaneously.

Photo 13: The delamination crack at the first interface stops.

Photo 15: The delamination crack at the second interface stops.

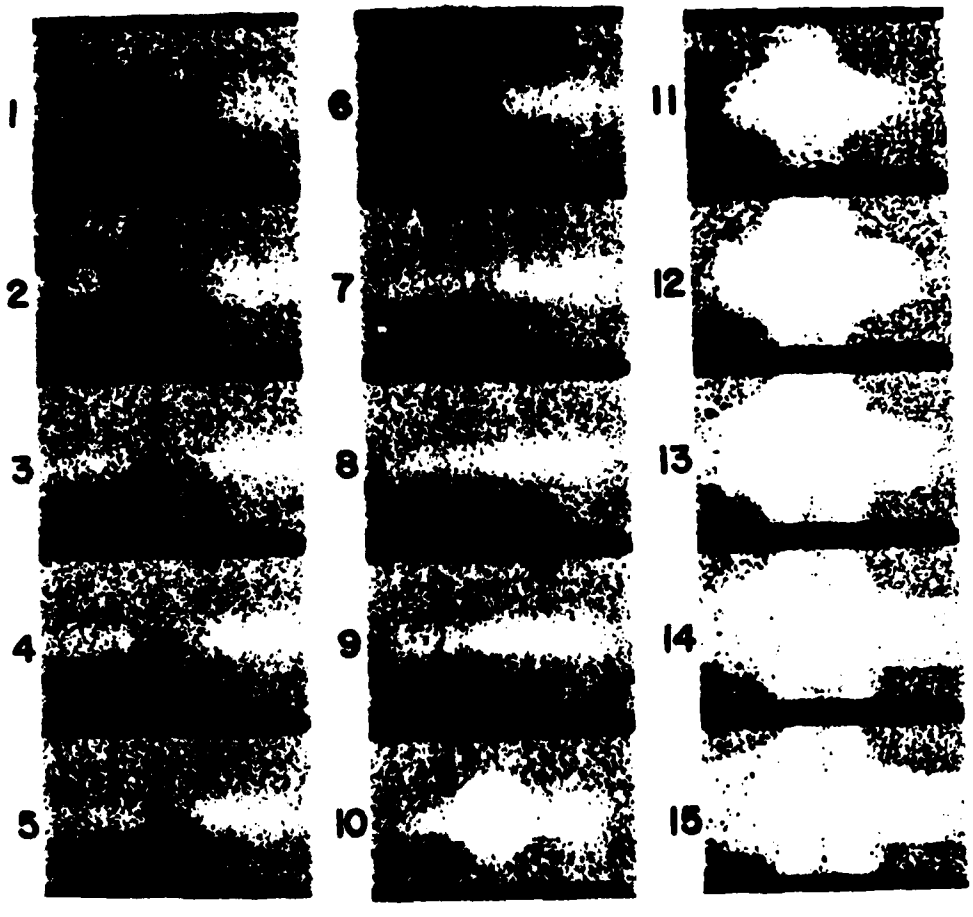

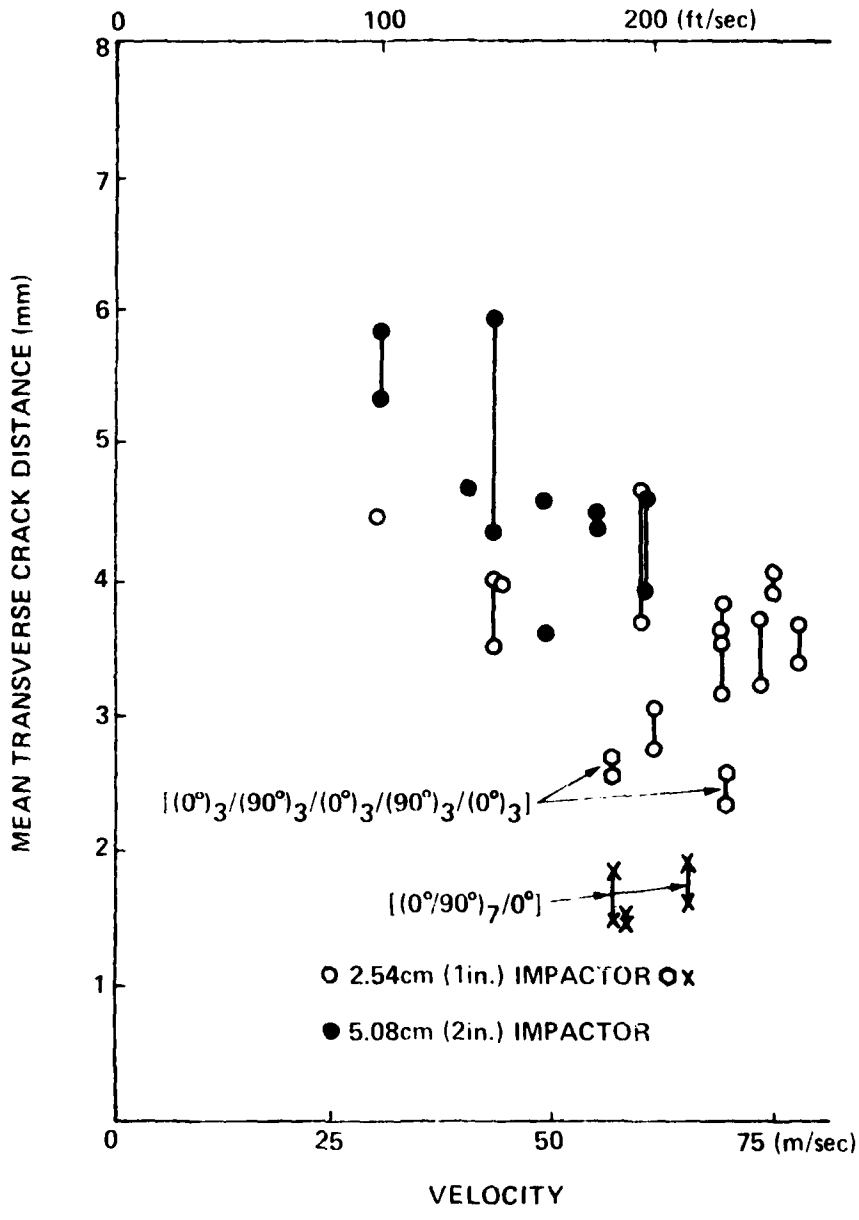

FIGURE 10. MEAN TRANSVERSE CRACK DISTANCE v.s. IMPACTOR VELOCITY FOR $[(0°)_5/(90°)_5/(0°)_5]$ LAMINATES IMPACTED BY A BLUNT NOSED IMPACTOR


DAT
ILM